Mapping Land-Use and Land-Cover Changes in Bahir Dar City and Its Surrounds Using Remote Sensing

Abel Balew Bimrew [a], Tesfaye Korme Oda [b]

[a] Abel Balew Bimrew
 Corresponding author
 Lecturer in Department of Geography and Environmental Studies, Madda Walabu University, Ethiopia. P.O.Box: 247 Bale Robe, Ethiopia; Email: abelbalew@gmail.com.

[b] Tesfaye Korme Oda
 Associate Professor in Ministry of Water, Electricity and Irrigation, Addis Ababa, Ethiopia; Email: tkorme@yahoo.co.uk.

Abstract

Spatio-temporal Land-Use and Land-Cover (LULC) changes have been affecting geo-environmental and climate change globally. This study aims to analyze LULC changes in Bahir Dar city and its surrounds. Landsat 5 TM (1987), Landsat 7 ETM+ (2002) and Landsat 8 OLI (2017) and SPOT images, and aerial photographs, master plan map and Google Earth Landsat images were used to analyze changes. In Bahir Dar city and its surrounds, LULC has been changing in space and time. During 1987-2017, more than 50% of the study area was covered with cropland. Settlement areas have increased from 3.3% in 1987 to 9.13% in 2017. However, wetland vegetation, shrubland, grassland, forest, and waterbodies have degraded. These changes are mainly attributed to population growth and its effect on the environment. Land-use and land-cover is a serious problem and it causes land and environmental degradation, climate change and loss of the biological environment.

Keywords: Landuse and landcover; LULC change; remote sensing; Bahir Dar city

1. Introduction

Currently, more than half of the world's population live in urban areas and this is expected to be 66% in the year 2050 (United Nations, 2014). Developing countries, especially Africa and Asia contribute more to this rapid increase of urbanization (UN-HABITAT, 2013, 2010). Rapid population growth in the urban area has been increasing land-use and land-cover (LULC) changes globally in magnitude and spatial extent (Defries et al., 2004; Hansen et al., 2013; Lambin et al.,

2001; Lambin and Meyfroidt, 2011; Mustard et al., 2012). As the population increases the demand for resource utilization increases proportionally and puts pressure on natural resources and damages them. Besides, the land has been continuously and extremely depleted due to anthropogenic factors (Brink et al., 2014; Niamir-Fuller et al., 2012) since people could not take care of their land. Therefore, rapid population growth exploits both natural and manmade resources (Bhattacharjee and Nayak, 2003; Sarma et al., 2008).

In Ethiopia, problems of LULC changes are very high and have been increasing from year to year. This is mainly due to population growth (Hurni et al., 2005) and perceptions of local communities towards land management systems (Belay et al., 2014) which contributes a lot of conversion of landscape and depletion of resources, for instance, forest and its biodiversity, water and soil resources. As a result, the country is vulnerable to surface runoff and flooding, and sedimentation (Hurni et al., 2005) which are associated with extreme land-cover degradation. The land is very dynamic in all parts of the country particularly in Amhara regional state the problem is very severe because the land is not sufficient to support the population of the region. Because of this, particularly forest, woodland, and shrubland land-covers have been heavily depleted to obtain additional land for settlement, farmland and grazing land. Therefore, these cause deforestation, loss of biodiversity, soil erosion and land degradation and raise climate change.

The patterns of land-use and the types of land-cover of Bahir Dar city and its surroundings have been changing due to rapid urbanization. As a result, land-covers like forest, woodland, bushland, wetland shrubland, and waterbodies have depleted drastically. These result in land degradation and its associated effects, urban climate change and affect the living conditions of people. Therefore, in order to ensure sustainable management LULC change and maintain climate changes it is very crucial to monitor paths of land-use and land-cover changes and its dynamism and predict their possible future conditions. The main goals of this study are: (1) to monitor land-use and land-cover of Bahir Dar city and its surrounding from 1987 to 2017; (2) to assess LULC changes in the city and its surrounding and examine effects of land-use and land-cover changes.

2. Role of Remote Sensing for Mapping Land-Use and Land-Cover Change

The land is becoming degraded and the pattern and types of land-cover are changing at local, regional and global levels. Therefore, efficient ways of analyzing what, why, where and when

land-use and land-cover are changed is essential for sustainable land management and economic development. Furthermore, assessing and mapping the consequences of LULC change and the possible solution is very significant. Monitoring temporal land-use and land-cover changes is also very important for environmental management.

In this regard, remote sensing has been playing a crucial role in providing satellite imagery to assess natural resources and monitor environmental changes. For example, Landsat is one of the satellites providing synoptic, repetitive and global coverage data freely since 1972. Landsat imagery have been used for various terrestrial applications. Therefore, remote sensing allows analysis land-use and land-cover change dynamics using time series of remotely sensed data by integrating it with socio-economic or biophysical data. Remote sensing is also efficient in land-cover mapping, detecting and monitoring land-cover change over time and space, identifying land use attributes and land cover change hot spots (Abate, 2011; Abbas et al., 2010; Temesgen et al., 2014). With the advancement of technology, reduction in data cost, availability of historic spatio-temporal data and high-resolution satellite images, remote sensing technologies are now very useful for conducting land cover change detection analysis and predicting future scenarios (Agarwal et al., 2002).

3. Data and Methods

3.1 Study Area

This research was conducted in Bahir Dar city and its surroundings which is the capital of Amhara National Regional State. Bahir Dar city is situated south of Lake Tana. The geographical location of the study area extends from latitude 11° 25' 19" to 11° 57' 7"N and longitude 37° 14' 35" to 37° 29' 7"E (Figure 1). It has a total area of 243.07 km^2, from which 215.57 km^2 is Bahir Dar city, and the remaining 27.41 km^2 and 0.09 km^2 was Deq Istifanos and Kibran Gebriel Islands, respectively). Besides, as estimated by CSA the population of the city could be 362,297 in 2017 (CSA, 2013).
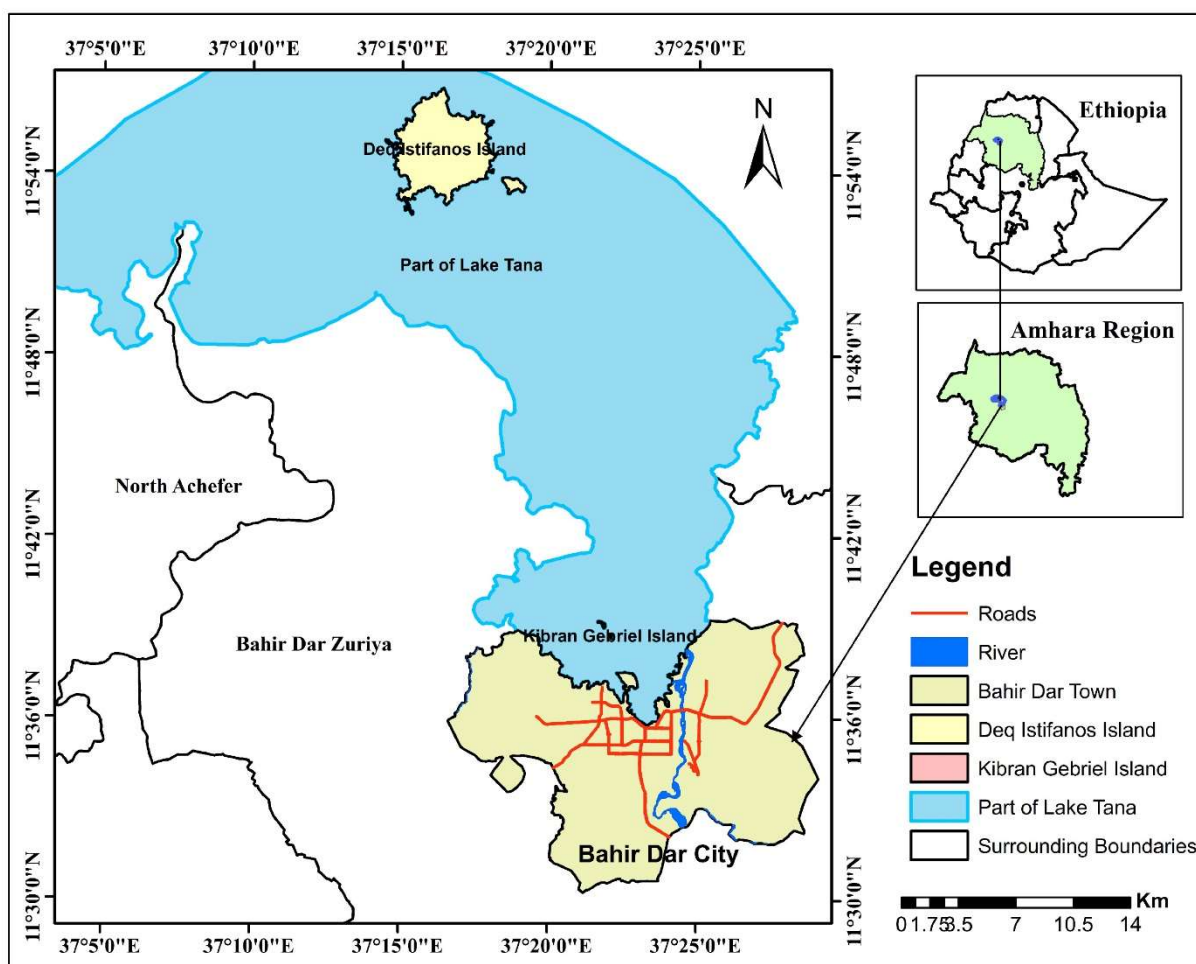
Figure 1: Geographical setting of the study area

3.2 Datasets

Landsat, SPOT, aerial photographs, master plan map and Google Earth Landsat images were the main datasets used for LULC classification and change detection analysis (Table 1). Images acquired by Landsat 5 TM, Landsat 7 ETM+ and Landsat 8 OLI scenes of the year 1987, 2002 and 2017, respectively were used. All these Landsat images were acquired during the month of March because cloud and haze free images can easily be obtained during dry seasons where there is no cloud cover and rain. These images were downloaded from the United States Geological Survey website (http://earthexplorer.usgs.gov). Images acquired by SPOT 5 HRG in the year 2005 were used for Landsat images sharpening. Google Earth Landsat images were used as a base map for LULC classification, particularly for the year 2017. However, Google Earth Landsat archive images for 1987 and 2002 are not visible and clear to develop LULC thematic layers. As a result,

to aid image classification for these two study years, aerial photographs and master plan map of the city in 2003 were used. Ground truth data collected from the field using GPS and Google Earth Landsat images were used to validate LULC thematic layers.

Table 1: Datasets used for the study and their source

Satellite	Sensors	Resolution (PAN/MS/TIRS)	Acquisition date	Source
Landsat 5	TM	15/30/120 m	27 March 1987	USGS
Landsat 7	ETM+	15/30/60 m	12 March 2002	
Landsat 8	OLI	15/30/100 m	13 March 2017	
SPOT 5	HRG	5 m	2005	EMA

3.3 Methods

3.3.1 Digital Image Preprocessing

In remote sensing, Digital Numbers (DN) represent reflectance of surface materials detected by a sensor and tells about the properties of an object. The objects are represented in the form of pixels (pictorial element). Therefore, digital image processing (DIP) should be done to obtain meaningful information from pixels. Digital image processing is helpful to maintain the quality image through minimize interpretation errors for the purpose of interpretation and classification. Thus, DIP techniques such as image layer stacking, sub-setting and image enhancement were done in ENVI 5.1 environment.

Image sharpening: is an image enhancement technique which helps to improve the resolution of the images and enhance image interpretation. Among many image sharpening techniques, Gram-Schmidt spectral sharpening algorithm was used to sharpen Landsat images using SPOT 5 images. The Gram-Schmidt method is typically more accurate because it uses the spectral response function of a given sensor to estimate what the panchromatic data look.

3.3.2 Radiometric Correction

Atmospheric image correction is very significant in order to get an accurate image because radiation which comes from the source always interacts with the atmosphere. Therefore, in atmospheric preprocessing, DN should be converted into spectral radiance. Digital numbers of TM and ETM+ images were converted into radiance using the equation (Markham and Barker, 1986):

$$L_\lambda = \left((LMAX_\lambda - LMIN_\lambda)\,/(QCALMAX - QCALMIN)\right) * (QCAL - QCALMIN) + LMIN_\lambda \quad (1)$$

Where: L_λ is spectral radiance received by the sensor (W/ (m^2 * sr * µm)), $QCAL$ is the quantized calibrated pixel value in DN, $LMIN_\lambda$ is the spectral radiance that is scaled to $QCALMIN$ (W/ (m^2 * sr * µm)), $LMAX_\lambda$ is the spectral radiance that is scaled to $QCALMAX$ (W/ (m^2 * sr * µm)), $QCALMIN$ is the minimum quantized calibrated pixel value (corresponding to $LMIN_\lambda$ in DN which is 1), $QCALMAX$ is the maximum quantized calibrated pixel value (corresponding to $LMAX_\lambda$ in DN which is 255).

Once DN is converted into radiance, the spectral radiance was converted to Top of Atmosphere (TOA) reflectance according to the equation:

$$\rho_\lambda = \frac{\pi * L_\lambda * d^2}{ESUN_\lambda * \cos\theta_{SZ}} \quad\quad\quad (2)$$

Where: ρ_λ is TOP reflectance (unitless), π is mathematical constant equals to ~ 3.14159 (unitless), L_λ is spectral radiance at the sensor's aperture (W/ (m^2 * sr * µm)), d is Earth-Sun distance (astronomical units), $ESUN_\lambda$ is mean exoatmospheric solar irradiance, θ_{SZ} is solar zenith angle (degree).

Digital numbers of Landsat 8 OLI image were also converted to radiance using the formula given by USGS (2016).

$$L_\lambda = M_\lambda Q_{cal} + A_L \quad\quad\quad (3)$$

Where: L_λ is spectral radiance (W/ (m^2 * sr * µm)), M_λ is radiance multiplicative scaling factor for the band (RADIANCE_MULT_BAND_N from the metadata), A_L is Radiance additive scaling factor for the band (RADIANCE_ADD_BAND_N from the metadata), Q_{cal} is level-1 pixel value in DN.

The spectral radiance received by the sensor is converted into TOA reflectance using the equation:

$$\rho_\lambda = \frac{M_\rho Q_{cal} + A_\rho}{cos\theta_{SZ}} \quad\quad\quad (4)$$

Where: ρ_λ is Top-of-Atmosphere Planetary Reflectance, θ_{SZ} is local solar zenith angle, M_ρ is reflectance multiplicative scaling factor for the band (REFLECTANCE_MULT_BAND_N from the metadata), A_ρ is reflectance additive scaling factor for the band (REFLECTANCE_ADD_BAND_N from the metadata), Q_{cal} is level-1 pixel value in DN.

3.3.3 Image Classification

Image classification is a technique of extracting information from image based on the reflectance value of an object (Gao, 2009; Lillesand et al., 2004; Richards and Jia, 2006). The information class can be grouped into a thematic layer of having similar LULC in the image. Though there are automated image classification techniques, manual or visual image interpretation procedures were used. This is because there is a problem of pixel mixing especially in low-resolution images such as Landsat and this has seriously affected the land-use and land-cover classification accuracy of the study. To aid visual image interpretation and maintain classification accuracy, Google Earth Landsat images, aerial photographs and Bahir Dar city master plan were used. Thus, to generate land-use and land-cover thematic layers, image digitizing and split and merge functions were employed in ArcGIS 10.5 environment.

3.3.4 Accuracy Assessment

Accuracy assessment is a comparison of image interpretation by a computer with the aid of ground truth data (Gao, 2009; Richards and Jia, 2006). For this comparison, training sites which used for accuracy assessment were identified based on the stratified method of sampling because the classified image has virtually been thematically stratified. Stratified sampling guarantees that a specified number of evaluation pixels can be selected from a given land cover, that is all LULC classes can be adequately represented in the evaluation samples. No matter how small a land cover is in size or limited in its spatial distribution, this specified number of evaluation pixels can always be selected, although not in a single pass (Gao, 2009). Therefore, stratified training pixels for validation were selected based on the number of bands and LULC classes, i.e., N(N + 1) is the formula used for taking the total samples for validation and for each LULC class (N+1) training pixels is required (Lillesand et al., 2004; Richards and Jia, 2006).

Based on the aforementioned formula, eight samples were taken for each thematic layer and 112 for all LULC classes for each study images (1987, 2002 and 2017). Using these training sites, each

LULC class of the study area was checked and its classification accuracy was assessed. The overall accuracy, producer's, and user's accuracy and kappa coefficient were calculated based on the error matrix derived from each classification result. The overall accuracy is defined as the proportion of correctly classified pixels divided by the total classified pixels, as illustrated in equation 5.

$$OA = \frac{\sum_{d=1}^{N} V_d}{\sum_{i=1}^{N} V_i} \qquad (5)$$

Where: N is the total number of classified pixels, $\sum_{d=1}^{N} V_d$ is the sum of diagonal (correctly classified) pixels and $\sum_{i=1}^{N} V_i$ is the sum of pixels along row.

Kappa coefficient was also calculated according to the equation given below.

$$\widehat{K} = \frac{N * \sum_{d=1}^{N} V_d - \sum_{ij=1}^{N}(x_i * x_j)}{N^2 * \sum_{ij=1}^{N}(x_i * x_j)} \qquad (6)$$

Where: $\widehat{K}$ is kappa coefficient, N is the total number of classified pixels x_i is total row pixel value for a certain class, x_j is total column pixel value for the same class.

3.3.5 Change Detection Analysis

Change detection is a process of detecting differences with the objects or phenomena which are observed in the different time intervals. DeltaCue is an application designed to help to identify changes of interest in remotely sensed imagery acquired on two dates. The DeltaCue change detection process operates on co-registered image data and performs a differencing operation as its core change detection process. In order to analyze the total area of LULC changed from 1987 to 2017, the following formula was used.

$$LULC\ change\ (\%) = \big(Area\ of\ recent\ year(\%) - Area\ of\ former\ year(\%)\big) \qquad (7)$$

4. Results and Discussion

4.1 Accuracy Assessment

Overall accuracy for 1987, 2002 and 2017 land-use and land-cover maps were 85.71%, 86.61%, and 92%, respectively. The Kappa coefficient agreement of classes and overall classification for the study periods were 0.854, 0.864 and 0.92, respectively as shown in (Table 2).

Table 2: Summary of accuracy assessment for 1987, 2002 and 2017

LULC Classes	1987	2002	2017
Overall Accuracy	85.71	86.61	92
$\widehat{K}$	0.854	0.864	0.92

4.2 Land-use and Land-cover during 1987-2017

Cropland was the dominant land-use class in 1987 (Table 3 & Figures 2-4). From the total study area, cropland accounted for 143.49 km^2 (59.03%). Whereas wetland vegetation, grassland, and shrubland accounted for 21.27 km^2 (8.75%), 19.17 km^2 (7.89%) and 18.06 km^2 (7.43%), respectively. In 1987, high-density settlements covered the smallest area (0.31 km^2).

Table 3: Land-use and land-cover classes and their area coverage in 1987, 2002 and 2017

| LULC Classes	1987		2002		2017	
	Area (km^2)	Area (%)	Area (km^2)	Area (%)	Area (km^2)	Area (%)
Cropland	143.49	59.03	146.58	60.3	122.63	50.45
Forest	7.53	3.1	4.62	1.9	4.43	1.82
Grassland	19.17	7.89	16.97	6.98	13.22	5.44
High density settlement	0.31	0.13	1.47	0.6	3.74	1.54
Industrial area	0.44	0.18	0.59	0.24	2.12	0.87
Low density settlement	7.70	3.17	11.14	4.58	18.44	7.59
Open space	6.72	2.76	8.13	3.34	13.27	5.46
Paved surface	0.61	0.25	0.71	0.29	1.45	0.6
Plantation	3.85	1.58	7.5	3.09	15.52	6.38
Riparian vegetation	0.67	0.28	0.66	0.27	0.67	0.28
Service area	9.21	3.79	12.42	5.11	17.23	7.09
Shrubland	18.06	7.43	10.58	4.35	9.39	3.86
Water body	4.04	1.66	4	1.65	3.91	1.61
Wetland vegetation	21.27	8.75	17.7	7.28	17.05	7.01
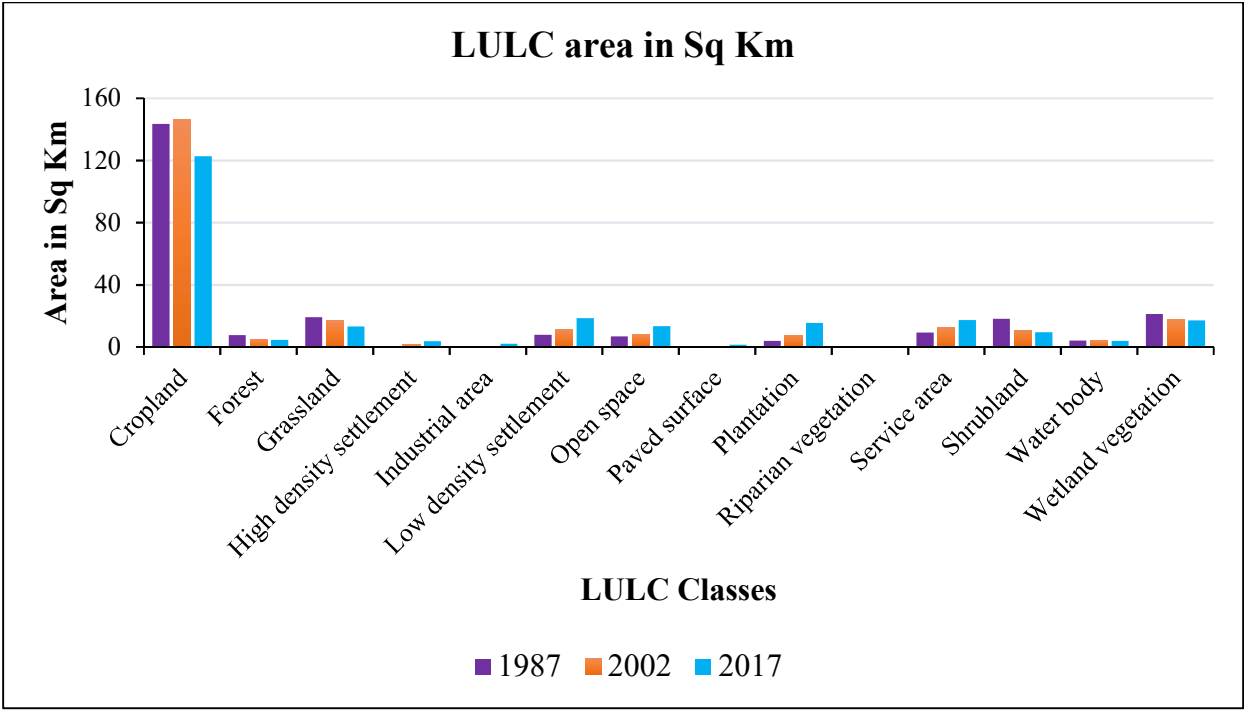
Figure 2: Land-use and land-cover *area* in km² (1987, 2002 & 2017)
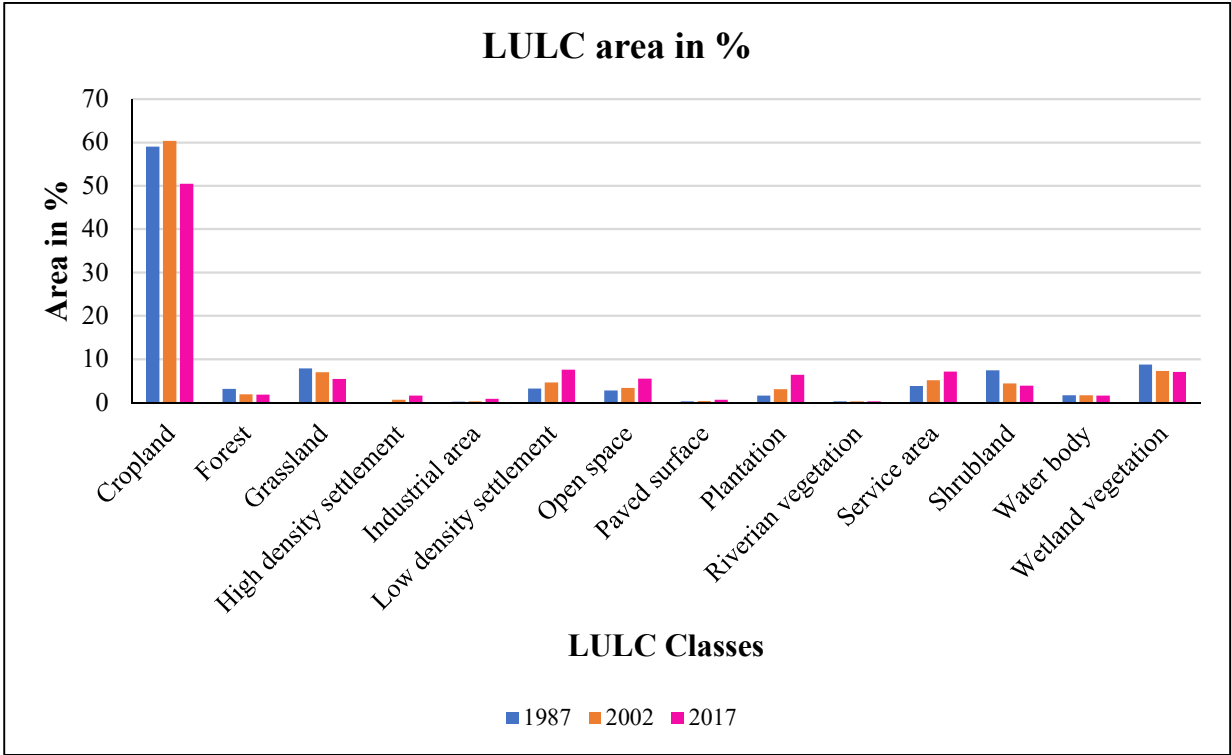

Figure 3: Land-use and land-cover area in % (1987, 2002 & 2017)

In 1987, most places in northeast, east, west, south, and southwest parts of Bahir Dar city and central Deq Istifanos Island were covered with cropland. Settlements, open space, paved surface, service, and industrial areas were concentrated in the center of the city. Service areas such as monasteries and churches were also found in Kibran Gebriel and Deq Istifanos Islands. Wetland vegetation cover was found along River Abay and Lake Tana shore, and some places in the west tip of the city. Most of the area of Kibran Gebriel Island was covered with forest. Forest cover was also found on Deq Istifanos Island and some places city. Grassland has covered some places in the center, west, southeast, eastern Bahir Dar and some places in eastern Deq Istifanos Island (Figure 4).
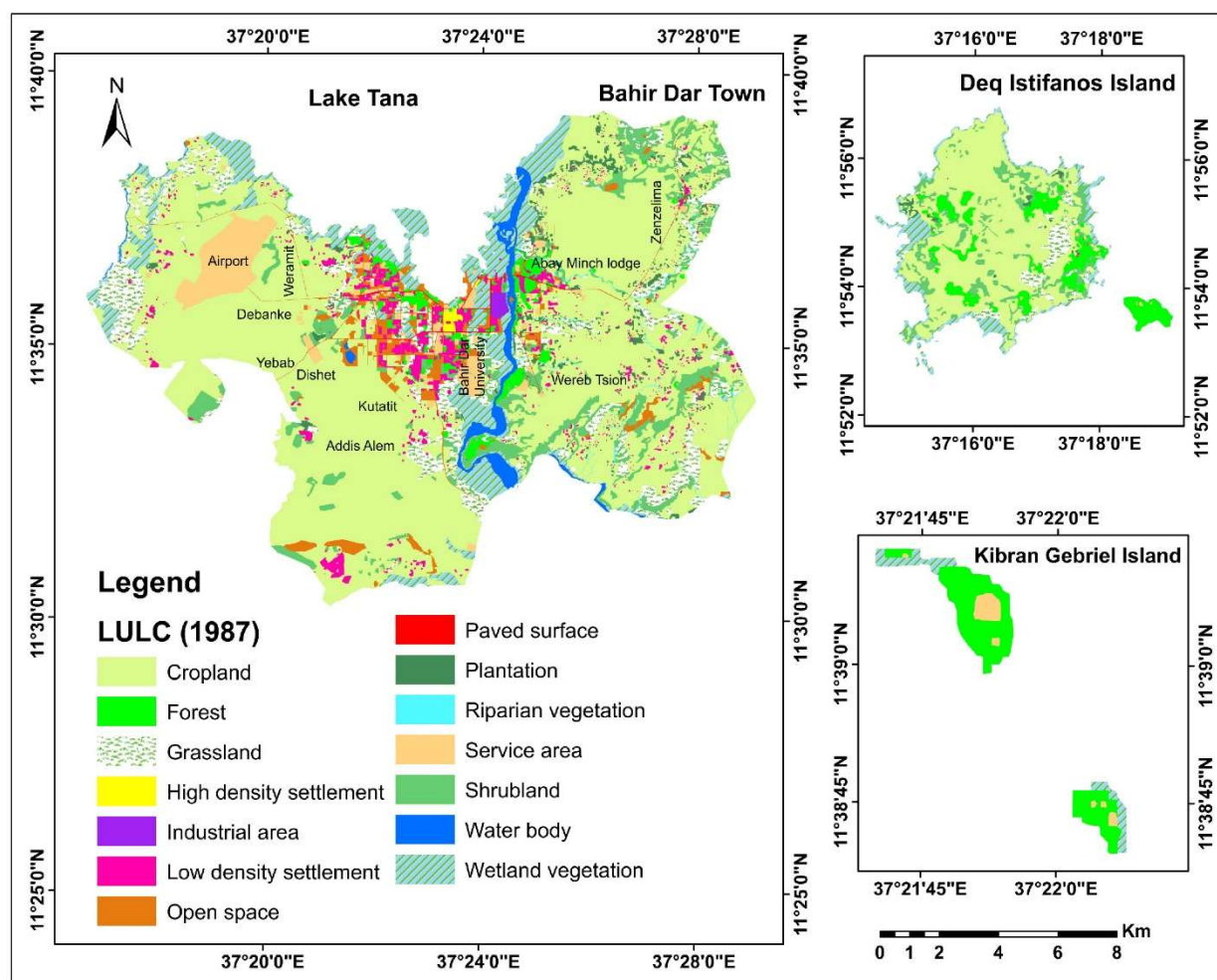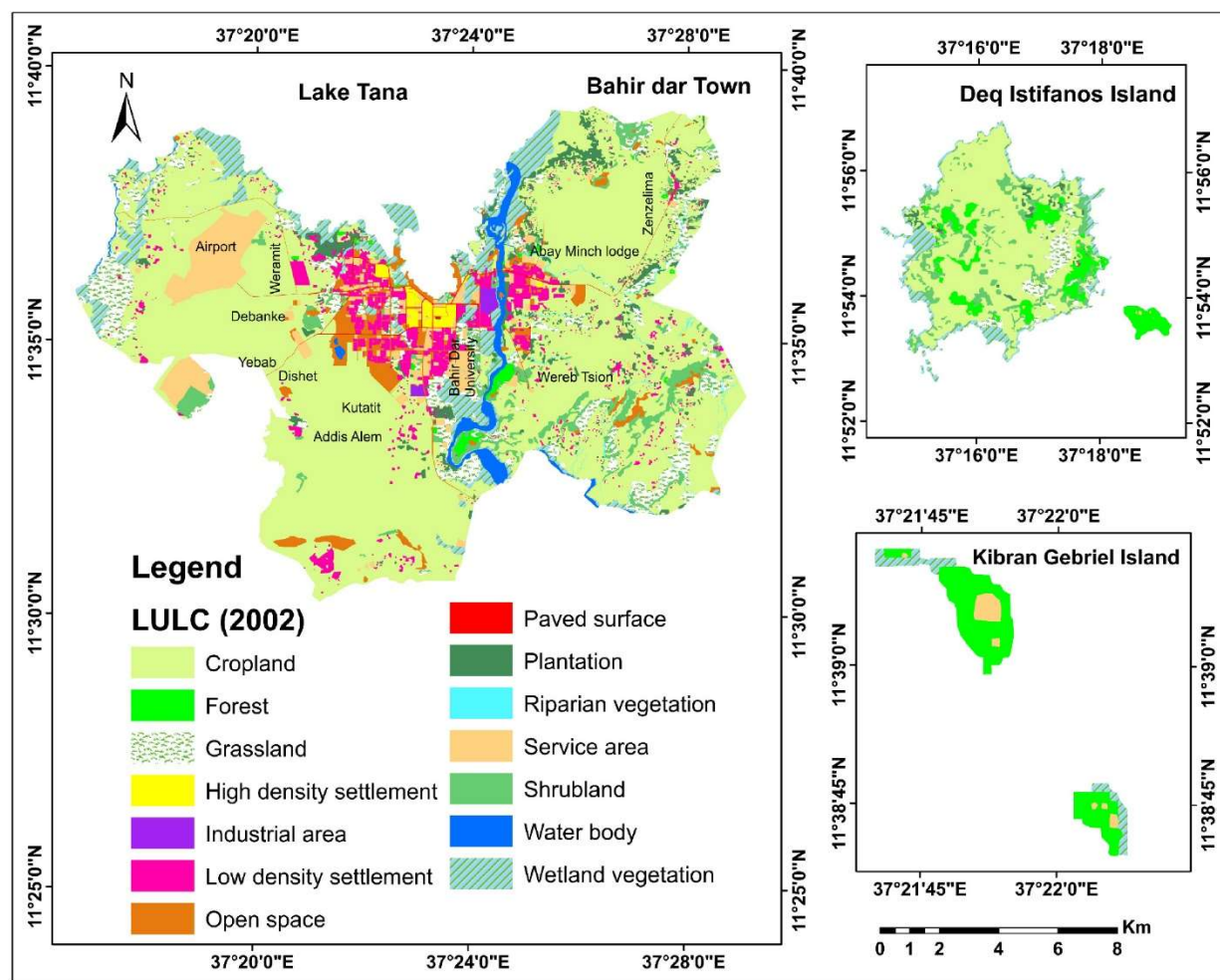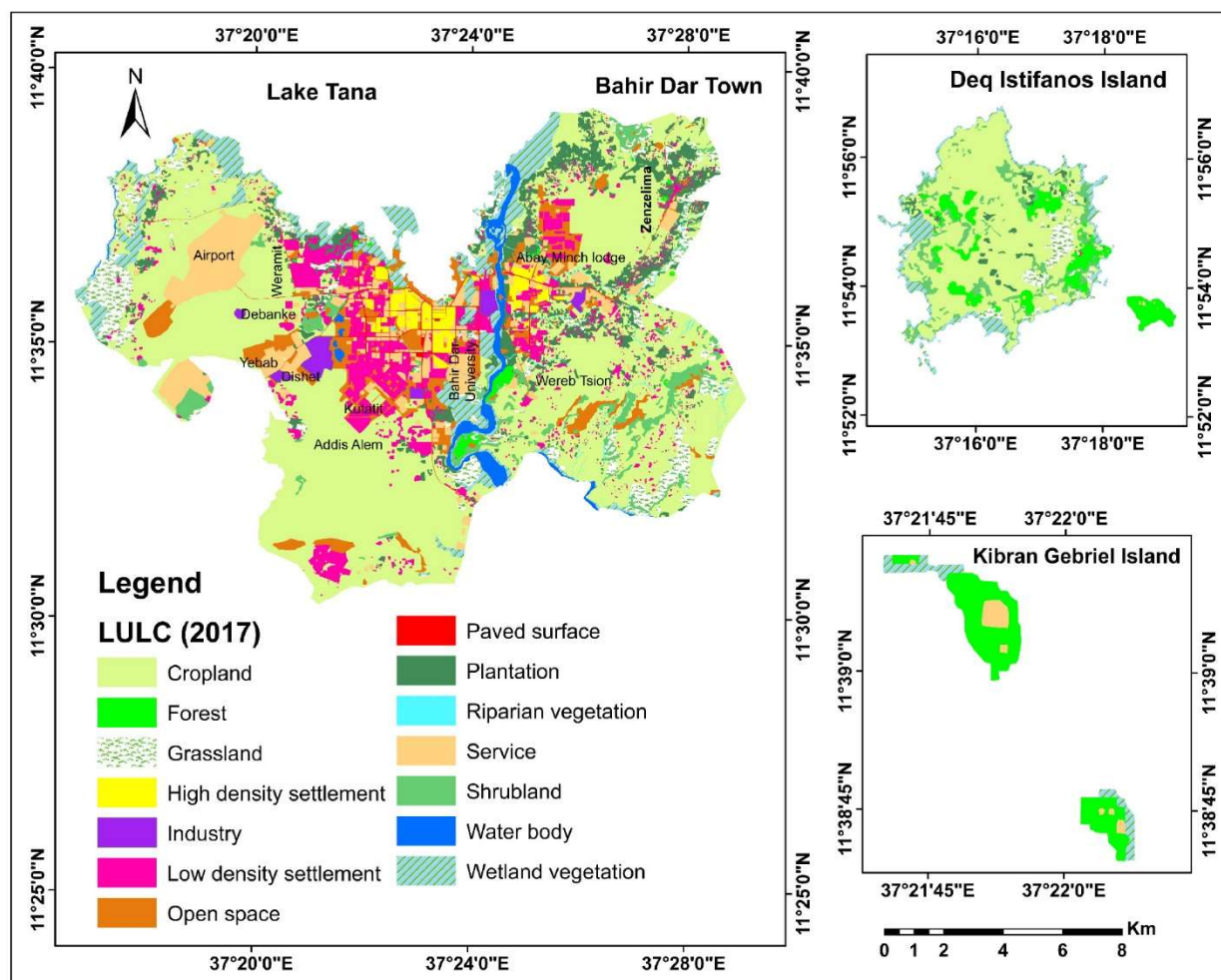

Figure 4: Land-use and land-cover map of 1987

In 2002, cropland covered an area of 146.58 km^2 (60.3%) (Table 3). It covered most eastern, west and southeastern Bahir Dar city and central Deq Istifanos Island (Figure 5). Wetland vegetation, grassland, service area, low density settlement, and shrubland land-use and land-cover classes also covered high area.

Figure 5: Land-use and land-cover map of 2002

Cropland was also the leading land-use and land-cover class in 2017 having an area of 122.63 km^2 (50.45%) though it has decreased by 23.95 (9.85%) from 2002. Low density settlement, service area, wetland vegetation, plantation and open space LULC classes have a high surface area next to cropland (Table 2 and Figures 6).

Figure 6: Land-use and land-cover map of 2017

### 4.3 Spatio-temporal Land-use and Land-cover Changes from 1987 to 2017

During 1987 to 2017, LULC in Bahir Dar city and its surrounding has changed in type, magnitude and spatial extent. Anthropogenic effects were the driving factors for such kinds of extreme changes (Agarwal et al., 2002; Brink et al., 2014; Niamir-Fuller et al., 2012). Cropland reduced from 143.49 km^2 (59.03%) in 1987 to 122.63 km^2 (50.45%) in 2017 with a negative net-change of 20.86 km^2 (8.58%). Landscape covered with shrubland, grassland, wetland vegetation, forest and waterbodies was also declined. Particularly, urban expansion contributes to the dramatic change of LULC (Fenglei et al., 2009; Jianga and Tiana, 2010). However, plantation, low-density settlement, service area, open space, high-density settlement, industrial area and paved surface have increased during 1987-2017. However, riparian vegetation has not changed during the study periods (Table 4 and Figures 7-10).

Table 4: Land-use and land-cover net-change from 1987 to 2017

LULC Classes	1987		2002		2017		Net-Change 1987-2002 (km²)	Net-Change (1987-2002) %	Net-change 2002-2017 (km²)	Net-change 2002-2017 %	Net-change 1987-2017 (km²)	Net-change 1987-2017 %
	Area km²)	Area (%)	Area (km²)	Area (%)	Area (km²)	Area (%)						
CL	143.49	59.03	146.58	60.30	122.63	50.45	3.09	1.27	-23.95	-9.85	-20.86	-8.58
FO	7.53	3.10	4.62	1.90	4.43	1.82	-2.91	-1.20	-0.19	-0.08	-3.1	-1.28
GL	19.17	7.89	16.97	6.98	13.22	5.44	-2.2	-0.91	-3.75	-1.54	-5.95	-2.45
HDS	0.31	0.13	1.47	0.60	3.74	1.54	1.16	0.48	2.27	0.93	3.43	1.41
IN	0.44	0.18	0.59	0.24	2.12	0.87	0.15	0.06	1.53	0.63	1.68	0.69
LDS	7.7	3.17	11.14	4.58	18.44	7.59	3.44	1.42	7.3	3.00	10.74	4.42
OP	6.72	2.76	8.13	3.34	13.27	5.46	1.41	0.58	5.14	2.11	6.55	2.69
PS	0.61	0.25	0.71	0.29	1.45	0.60	0.1	0.04	0.74	0.30	0.84	0.35
PL	3.85	1.58	7.5	3.09	15.52	6.38	3.65	1.50	8.02	3.30	11.67	4.80
RV	0.67	0.28	0.66	0.27	0.67	0.28	-0.01	0.00	0.01	0.00	0	0.00
SA	9.21	3.79	12.42	5.11	17.23	7.09	3.21	1.32	4.81	1.98	8.02	3.30
SH	18.06	7.43	10.58	4.35	9.39	3.86	-7.48	-3.08	-1.19	-0.49	-8.67	-3.57
WB	4.04	1.66	4	1.65	3.91	1.61	-0.04	-0.02	-0.09	-0.04	-0.13	-0.05
WV	21.27	8.75	17.7	7.28	17.05	7.01	-3.57	-1.47	-0.65	-0.27	-4.22	-1.74

Where: CL=cropland, FO= forest, GL=grassland, HDS=high density settlement, IN=industrial area, OP=open space, PL=plantation, PS=paved surface, RV=riparian vegetation, SA=service area, SH=shrubland, LDS=low density settlement, WB=water body, WV=wetland vegetation
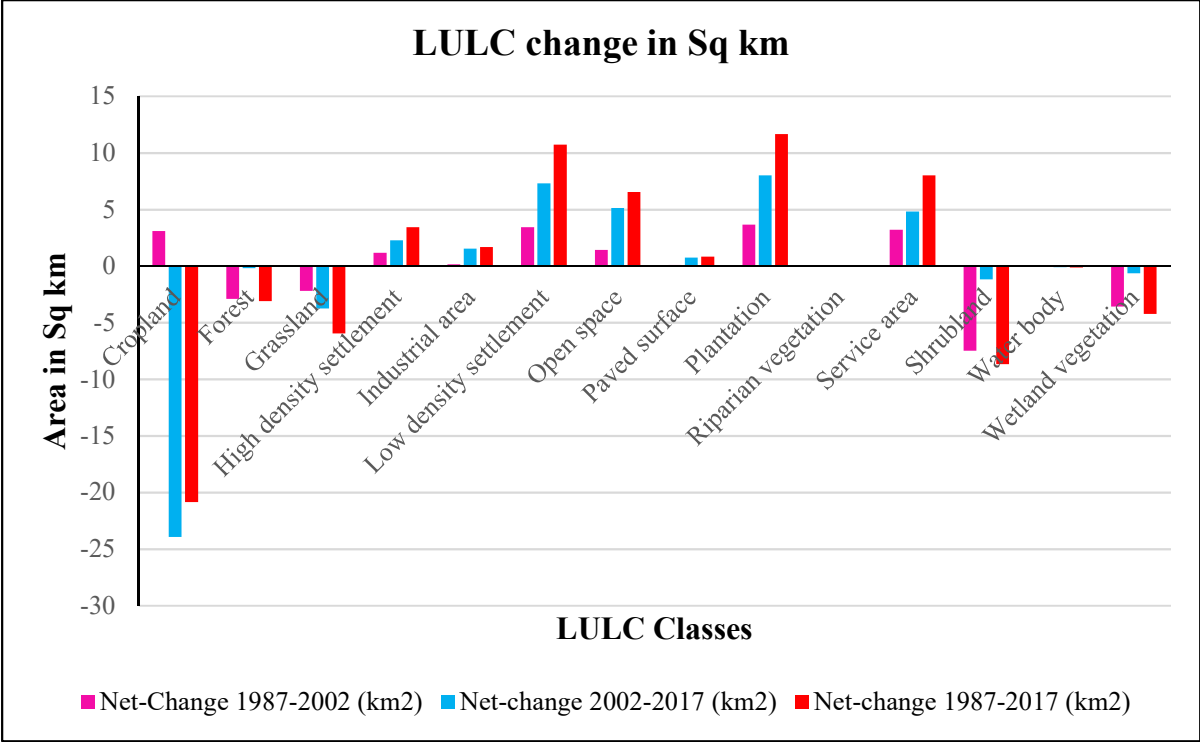
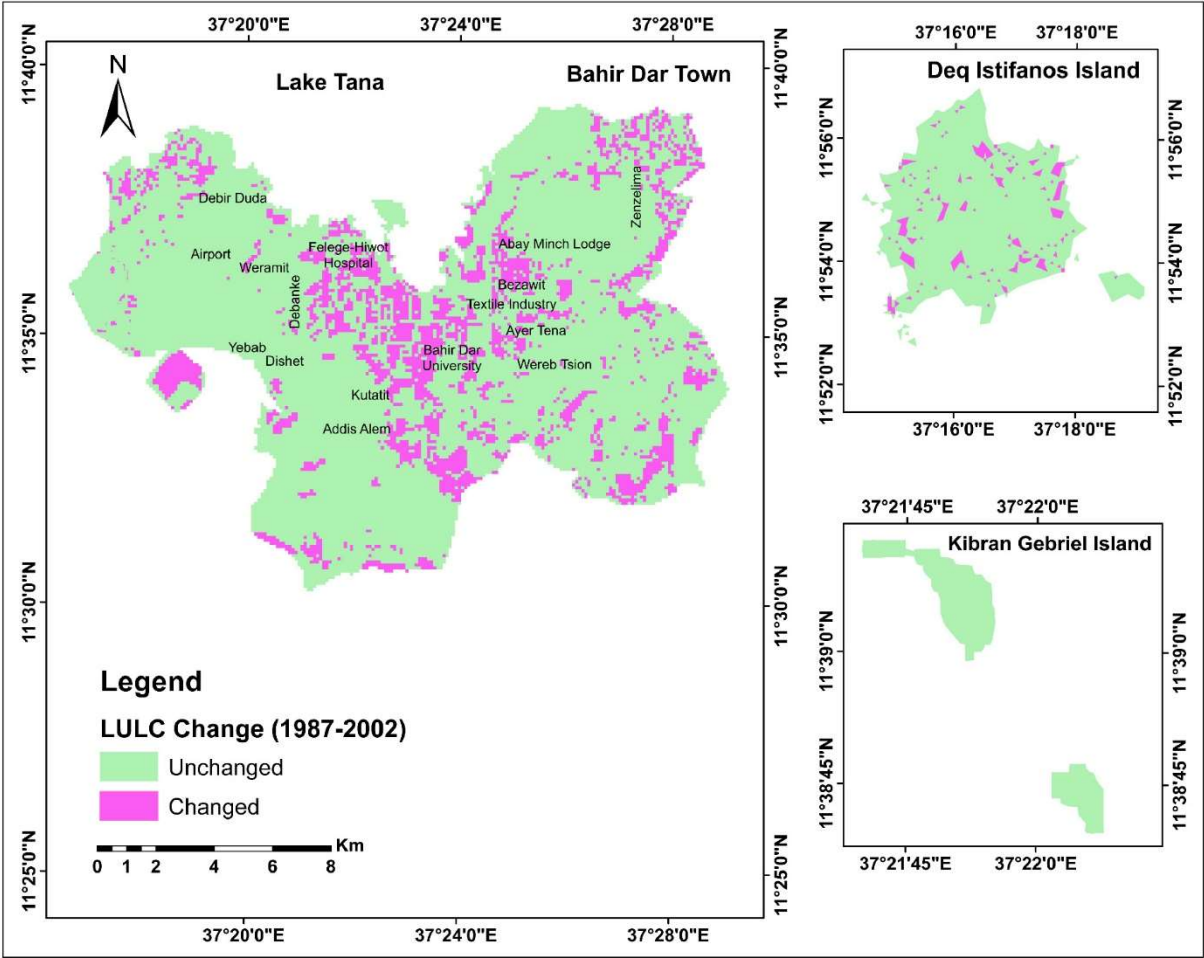**Figure 7: Land-use and land-cover change in km² (1987, 2002 & 2017)**

Figure 8: Land-use and land-cover change map from 1987-2002
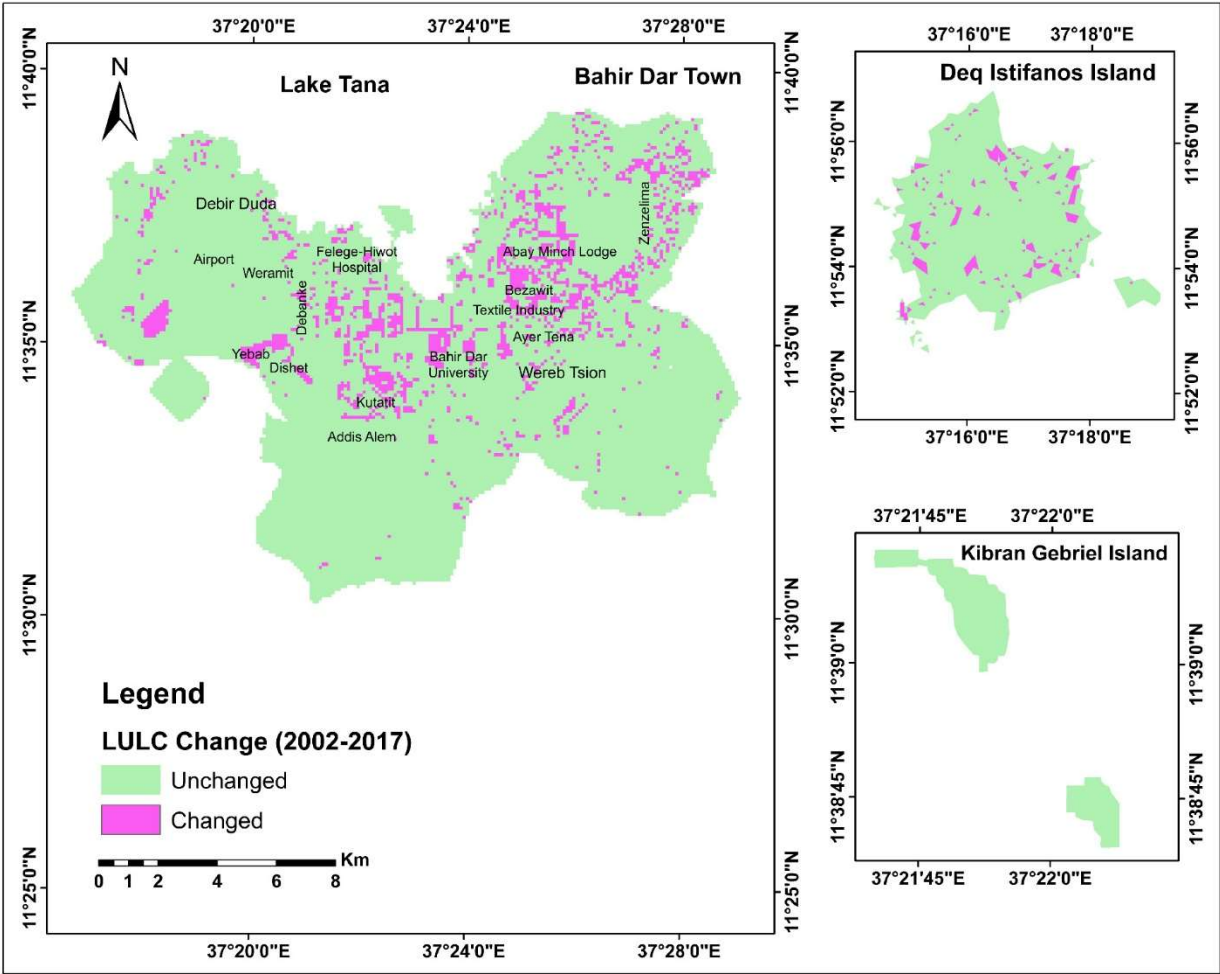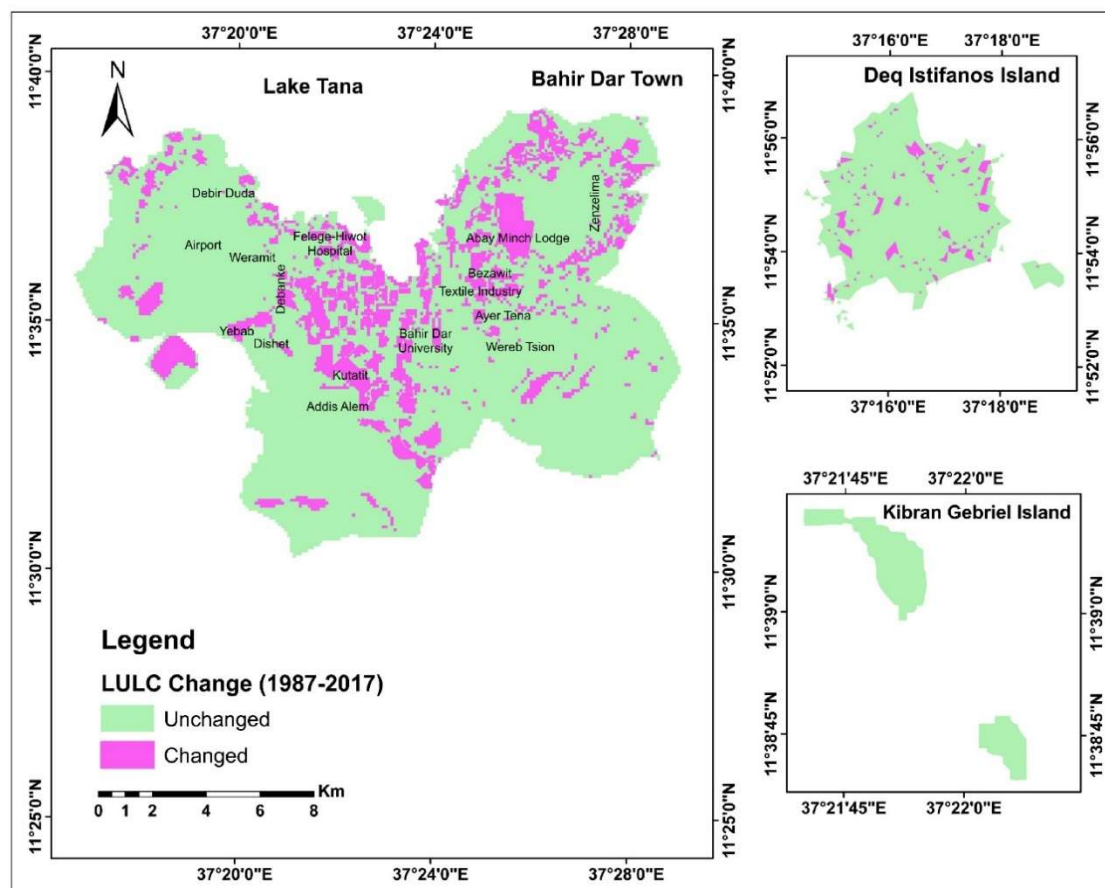
Figure 9: Land-use and land-cover changes map from 2002-2017

Figure 10: Land-use and land-cover changes map from 1987-2017

During 1987-2002, from total cropland change, 2.03 km^2 and 1.79 km^2 were converted into service area and low-density settlement, respectively. Cropland was also converted into plantation, open space, and grassland. Contrary to this, 5.35 km^2 cropland area was gained from shrubland in 2002. Shrubland also changed to grassland, open space, plantation, service, and low-density settlement. Furthermore, 3.33 km^2 of grassland were converted to cropland in 2002. Grassland was also changed to high and low-density settlement, open space, plantation, service area, and cropland. Wetland vegetation was converted to cropland, service area, open space, low-density settlement, grassland, plantation, and shrubland. Forest cover was also changed into low and high-density settlement, plantation, service area, cropland, open space, shrubland, and grassland. In addition, water body receded in 1987 and the area was covered with wetland vegetations (bushland and grassland) in 2002. Details about land-use and land-cover transformation matrix from 1987-2002 are illustrated in Table 5.

Table 5: Land-use and land-cover changes matrix from 1987 to 2002 (in km²)

LULC Class	LULC 2002														
	CL	FO	GL	HDS	IN	OP	PL	PS	RV	SA	SH	LDS	WB	WV	Class Total
CL	**136.32**	0.03	0.02			1.39	1.94			2.03		1.79			143.49
FO	0.25	**4.59**	0.07	0.34		0.22	0.33			0.30	0.15	1.28			7.53
GL	3.33		**14.72**	0.06		0.26	0.39			0.22		0.14		0.05	19.17
HDS				**0.31**											0.31
IN					**0.44**										0.44
OP	0.01			0.10	0.15	**5.38**	0.02	0.12		0.40		0.53			6.72
PL	0.02						**3.82**								3.85
PS						0.04		**0.57**							0.61
RV									**0.66**						0.67
SA				0.08						**9.13**					9.21
SH	5.35		1.02			0.37	0.61			0.13	**10.34**	0.24			18.06
LDS				0.57						0.07		**7.04**			7.7
WB													**3.98**	0.05	4.04
WV	1.30		1.14			0.49	0.39			0.14	0.10	0.11		**17.62**	21.27
Class Total	146.58	4.62	16.97	1.47	0.59	8.13	7.50	0.71	0.66	12.42	10.58	11.14	4	17.7	**243.07**

Where: CL=cropland, FO= forest, GL=grassland, HDS=high density settlement, IN=industrial area, OP=open space, PL=plantation, PS=paved surface, RV=riparian vegetation, SA=service area, SH=shrubland, LDS=low density settlement, WB=water body, WV=wetland vegetation

LULC 1987 *(row axis label)*

From the total cropland change during 2002-2017, 7.88 km^2, 7.59 km^2, 5.43 km^2, respectively were converted to low-density settlement, plantation, open space (Table 6). Cropland also converted into service and industrial areas, grassland, high-density settlement, wetland vegetation, and paved surface. Further, places covered with grassland in 2002 was altered to open space (1.58 km^2) and cropland (0.82 km^2) in 2017. Service area, plantation, low-density settlement, shrubland, high-density settlement, and wetland vegetation also expanded at the expense of grassland in 2017. Shrubland also changed into open space, plantation, cropland, service area, grassland, low-density settlement, forest and wetland vegetation. Moreover, wetland vegetation areas in 2017 were reduced due to the expansion of open space, grassland, cropland, plantation, service area, low and high-density settlement. During 2002-2017, forest cover was converted to plantation, service area, open space, low-density settlement, and shrubland. Areas covered with waterbodies in 2002 were converted to wetland vegetation and plantation in 2017. Table 6 presents detailed information of land-use and land-cover change from 2002 to 2017.

Table 6: Land-use and land-cover changes matrix from 2002 to 2017 (in km²)

LULC Classes	LULC 2017														
	CL	FO	GL	HDS	IN	OP	PL	PS	RV	SA	SH	LDS	WB	WV	Class Total
CL	**121.10**		0.19	0.04	1.33	5.43	7.59	0.01		2.95	0.03	7.88		0.03	146.58
FO		**4.41**				0.04	0.06			0.04	0.03	0.04			4.62
GL	0.82		**12.65**	0.14		1.58	0.54			0.54	0.22	0.45		0.04	16.97
HDS				**1.47**											1.47
IN					**0.59**										0.59
OP	0.09		0.03	0.15	0.20	**4.99**	0.04	0.74		0.76		1.04	0.10	0.01	8.13
PL	0.06		0.01			0.09	**6.66**			0.11	0.02	0.54			7.50
PS								**0.69**							0.71
RV									**0.66**						0.66
SA							0.01			**12.40**		0.01			12.42
SH	0.31	0.02	0.07			0.51	0.43			0.12	**9.04**	0.07		0.01	10.58
LDS	0.25			2.00		0.36	0.05	0.01		0.22	0.05	**8.19**			11.14
WB							0.02		0.01				**3.78**	0.17	4
WV	0.12		0.26	0.01		0.28	0.12			0.09		0.02		**16.81**	17.7
Class Total	122.63	4.43	13.22	3.74	2.12	13.27	15.52	1.45	0.67	17.23	9.39	18.44	3.91	17.05	**243.07**

Where: CL=cropland, FO= forest, GL=Grassland, HDS=high density settlement, IN=industrial area, OP=open space, PL=plantation, PS=paved surface, RV=riparian vegetation, SA=service area, SH=shrubland, LDS=low density settlement, WB=water body, WV=wetland vegetation

During 1987-2017, low and high-density settlements, industrial and service areas, open space, plantation, and paved surface were expanded at the expense of cropland, grassland, shrubland, forest, wetland vegetation and water body. Land-use and land-cover change matrix of Bahir Dar town and its surrounding from 1987-2017 is illustrated in Table 7.

Table 7: Land-use and land-cover changes matrix from 1987 to 2017 (in km²)

	LULC Class	LULC 2017														
		CL	FO	GL	HDS	IN	OP	PL	PS	RV	SA	SH	LDS	WB	WV	Class Total
LULC 1987	CL	**113.45**	0.01	0.19	0.32	1.47	5.77	7.70	0.02		5.05	0.03	9.52			143.49
	FO	0.02	**4.40**	0.02	1.17		0.31	0.37			0.42	0.15	0.64			7.53
	GL	3.23		**11.04**	0.22		1.73	1.25	0.03		0.78	0.06	0.81		0.01	19.17
	HDS				**0.31**											0.31
	IN					**0.44**										0.44
	OP				0.24	0.16	**3.61**	0.02	0.75		0.84		0.99	0.10	0.01	6.72
	PL	0.05					0.04	**3.54**			0.05		0.17			3.85
	PS								**0.61**							0.61
	RV									**0.67**						0.67
	SA				0.08						**9.12**					9.21
	SH	4.64	0.02	0.82	0.08	0.06	0.71	1.78			0.38	**9.09**	0.49		0.01	18.06
	LDS	0.24			1.34		0.26	0.05	0.01		0.27	0.05	**5.47**			7.69
	WB							0.02						**3.78**	0.21	4.04
	WV	1.15		1.15	0.04		0.85	0.78	0.02		0.32		0.15		**16.82**	21.27
	Class Total	122.63	4.43	13.22	3.74	2.12	13.27	15.52	1.45	0.67	17.23	9.39	18.44	3.91	17.05	**243.07**

Where: CL=cropland, FO= forest, GL=grassland, HDS=high density settlement, IN=industrial area, OP=open space, PL=plantation, PS=paved surface, RV=riparian vegetation, SA=service area, SH=shrubland, LDS=low density settlement, WB=water body, WV=wetland vegetation

4.4 Effects of Land-use and Land-cover Change

Land-use and land-cover changes occurred due to natural and anthropogenic factors. As the United States Environmental Protection Agency (EPA) (1999) states, there were three main driving grounds for land-use and land-cover changes. These are (1) natural processes, such as wildfire, climate and atmospheric changes, and pest infestation; (2) direct effects of human activity such as deforestation, soil erosion and reduction of biodiversity which brings land degradation, and construction like road and buildings.; and (3) indirect effects of human activities, like depletion or lowering of water table and contamination of groundwater.

Anthropogenic factors are the major driving forces of land-use and land-cover changes (Brink et al., 2014; Niamir-Fuller et al., 2012) even though there is also a contribution from the natural processes. Land-use and land-cover change is a very complex process (Abate, 2011; Belay, 2002) because its causes and impacts are very closely related; for example, land degradation. Currently, the human-related causes of land-use and land-cover changes are very serious (Agarwal et al., 2002).

Extreme land-use and land-cover change attributed to rapid population growth and expansion of agricultural land responsible for massive collapse of natural vegetation, loss of biodiversity and land degradation. Exhausted land is also vulnerable to soil erosion which causes declining of organic matter in the soil, soil structure degradation and reduction in soil nutrients. Extreme land degradation has a severe impact on the productivity of agricultural fields (Aadil et al., 2014). Extreme alteration of vegetation covers such as forests, grassland, wetlands, bushland and shrubland brings a reduction of biodiversity and endless degradation of the natural environment. Intensification of agriculture such as crop and pastoral land towards the natural ecosystem which is related to population growth also contribute towards extreme changes of LULC and environment (Lambin and Meyfroidt, 2011).

Moreover, landscape changes affect ecosystems and climate change. Deforestation also affects the process of atmosphere and thermodynamics at the earth-atmosphere interface and water storage capacity and soil hydraulic conductivity. Besides, changes in land-use and land-cover affect hydrological cycles and its parameters (Shukla et al., 1990; Zhenglei et al., 2009). Land-use and land-cover changes also cause wetlands degradation which strongly influence hydrological cycles

(Yanagi, 2008; Zhao and Lai, 2007), and this brings environmental change. The change in hydrological condition of the earth surface alters the physicochemical property of wetlands. The scarcity of water, drop of the freshwater source and depletion of the existing groundwater are also problems related to land-use and land-cover changes. These directly or indirectly affect food production, human health, and economic development (Zhenglei et al., 2009).

Moreover, exhaustive use of land and change of land-cover and its patterns vulnerable to soil and land degradation. This leads to increasing poverty and migration, failure of land productivity, damage of biodiversity and natural resources, deterioration of groundwater recharge and carbon storage capacity, and change in population size; and spatial distribution (Abate, 2011). Land-use and land-cover changes also have consequences of soil and land degradation, soil erosion, salinization and desertification. Soil and land degradation results in soil erosion, salinization, compaction, acidification, nutrient impoverishment, waterlogging and dehumification. Desertification is also another effect of extreme land-use and land-cover. It increases the concentration of carbon-di-oxide in the atmosphere and brings wildfire. Therefore, incidences of forest fire related to land-use and land-cover degradation/change increase the emission of toxic gases (GHG) such as carbon monoxide and nitric oxide which alter the chemistry of the atmosphere causing air pollution, affecting energy balance and climate and global warming. Land-use and land-cover change have impacts on hydrology. It changes the quality of water and water flows, cause surface water pollution, depletion of groundwater aquifers. Land-use and land-cover changes also increase the frequency and severity of flooding which is due to continuous and serious deforestation.

In addition, LULC change attributed to urban expansion causes dramatic changes in landscape patterns and types. This dynamic has been changing the availability of different biophysical resources and lead to decreased availability of different products and services for human, livestock, and damage the environment (Hussien, 2009). Therefore, extreme changes of landscape pattern around urban areas and the surroundings has massive impacts on the environment for instance urban heat island and pollution. This affects the living condition of people.

5. Conclusions

Remote sensing is very significant for assessing and mapping land-use and land-cover changes. Landsat images provides crucial information about the current conditions of land-use and land-cover, landscape dynamics and environmental changes. The land-use and land-cover of Bahir Dar city and its surrounds has been changing in space and time because of rapid population growth associated with exploitation of land-cover and urbanization. Extreme land-use and land-cover changes bring land and environmental degradation, destruction of ecological environment and climate change and urban heat islands.

Declarations of interest

There is no conflict of interest between the authors.

Submission Declaration

I hereby declare that this manuscript has not published previously and not submitted for any journal.

References

Abate, S. (2011). Evaluating the land use and land cover dynamics in Borena Woreda of South Wollo highlands, Ethiopia. J. Sustain. Dev. Afr., 13, 87–105.

Agarwal, C., Green, G.M., Grove, J.M., Evans, T.P., Schweik, C.M. (2002). A Review and assessment of land-use change models: Dynamics of space, time, and human choice. General technical report NE-297. Newtown Square, Pennsylvania: U.S. Department of Agriculture, Forest Service, Northeastern Research Station.

Belay, S., Amsalu, A., Abebe, E. (2014). Land use and land cover changes in Awash National Park, Ethiopia: impact of decentralization on the use and management of resources. Open J. Ecol., 4, 950–960.

Bhattacharjee, P.R., Nayak, P. (2003). Socio-economic rationale of a regional development council for the Barak Valley of Assam. J. NEICSSR, 27, 13–26.

Brink, A.B., Bodart, C., Brodsky, L., Defourney, P., Ernst, C., Donney, F., Lupi, A., Tuckova, K. (2014). Anthropogenic pressure in East Africa: Monitoring 20 years of land cover changes by means of medium resolution satellite data. Int. J. Appl. Earth. Obs. Geoinform., 28, 60–69.

CSA. (2013). Population projection of Ethiopia for all regions at wereda level from 2014 – 2017. Federal Democratic Republic of Ethiopia Central Statistical Agency, Addis Ababa, Ethiopia.

Defries, R.S., Foley, J.A., Asner, G.P. (2004). Land-use choices: Balancing human needs and ecosystem function. Front Ecol Env., 2, 249–257.

Donato, S.L.M.V., Sebastiano, C., Sebastiano, S., Federico, G.M. (2016). Anthropogenic influences in land use/land cover changes in Mediterranean forest landscapes in Sicily. Land 5. https://doi.org/doi:10.3390/land5010003

Fenglei, F., Yunpeng, W., Maohui, Q., Zhishi, W. (2009). Evaluating the temporal and spatial urban expansion patterns of Guangzhou from 1979 to 2003 by Remote Sensing and GIS methods. Int. J. Geogr. Inf. Sci., 23, 1371–1388.

Gao, J. (2009). Digital analysis of remotely sensed imagery. McGraw-Hill.

Hansen, M.C., Potapov, P.V., Moore, R., Hancher, M., Turubanova, S.A., Tyukavina, A., Thau, D., Stehman, S.V., Goetz, S.J., Loveland, T.R. (2013). High-Resolution Global Maps of 21st-Century Forest Cover Change. Science, 342, 850–853.

Hurni, H., Kebede, T., Gete, T. (2005). The implication of changes in population, land use and land management for surface runoff for Upper Nile Basin area of Ethiopia. Mt. Res. Dev., 25, 147–154.

Hussien, A.O. (2009). Land use and land cover change, drivers and its impact: A comparative study from Kuhar Michael and Lenche Dima of Blue Nile and Awash Basins of Ethiopia (A MScThesis). Cornell University, Ethiopia.

Jianga, J., Tiana, G. (2010). Analysis of the impact of land use/land cover change on land surface temperature with Remote Sensing. Procedia Environ. Sci., 2, 571–575.

Lambin, E.F., Meyfroidt, P. (2011). Global land use change, economic globalization, and the looming land scarcity. Proc Natl Acad Sci USA, 108, 3465–3472.

Lambin, E.F., Turner, B.L., Geist, H.J., Agbola, S.B., Angelsen, A., Bruce, J.W., Coomes, O.T., Dirzo, R., Fischer, G., Folke, C. (2001). The causes of land-use and land-cover change: Moving beyond the myths. Glob Env. Chang., 11, 261–269.

Lillesand, T.M., Kiefer, R.W., Chipman, J.W. (2004). Remote sensing and image interpretation, 5th ed. John Wiley & Sons, New York.

Liu, H., Zhang, S., Li, Z., Lu, X., Yang, Q. (2004). Impacts on wetlands of large-scale land-use changes by agricultural development: the small Sanjiang plain, China. Ambio, 33, 306–310.

Liu, Y., Zha, Y., Ni, S. (2004). Assessment of grassland degradation near Lake Qinghai, West China, using Landsat TM and in situ reflectance spectra data. Int. J. Remote Sens., 25, 4177–4189.

Markham, B.L., Barker, J.L. (1986). Landsat-MSS and TM post calibration dynamic ranges, atmospheric reflectance and at-satellite temperature. EOSAT Landsat Technical Notes 1, (Lanham, Maryland: Earth Observation Satellite Company), pp. 3–8.

Mustard, J.F., Defries, R.S., Fisher, T., Moran, E. (2012). Land-use and land-cover change pathways and impacts. Land Change Sci. Springer Dordr. Neth. 411–429.

Niamir-Fuller, M., Kerven, C., Reid, R., Milner-Gulland, E. (2012). Co-existence of wildlife and pastoralism on extensive rangelands: Competition or compatibility? Pastor Res Policy Pr. 2, 1–14.

Qijiao, X., Zhixiang, Z. (2015). Impact of urbanization on urban heat island effect based on TM imagery in Wuhan, China. Environ. Eng. Manag. J., 14, 647–655.

Richards, J.A., Jia, X. (2006). Remote sensing digital image analysis: An introduction, 4th ed. Springer-Verlag Berlin Heidelberg 2006, Germany.

Sarma, P.K., Lahkar, B.P., Ghosh, S., Rabha, A., Das, J.P., Nath, N.K., Brahama, N. (2008). Land use and Land cover change and future implication analysis in Manas National Park, India using multi temporal satellite data. Curr. Sci., 95, 1–5.

Tang, Z., Shi, C.B., Bi, K.X. (2014). Impacts of land cover change and socioeconomic development on ecosystem service values. Environ. Eng. Manag. J., 13, 2697–2705.

UN-HABITAT. (2013). State of the World's Cities 2012/2013: Prosperity of Cities. Routledge Taylor & Francis Group, United Nations Human Settlements Programme, New York.

UN-HABITAT (2010). State of the World's Cities 2010/2011: Prosperity of Cities. Earthscan, UK, United Nations Human Settlements Programme.

United Nations (2014). World urbanization prospects: The 2014 Revision, Highlights (No. ST/ESA/SER.A/352). United Nations, Department of Economic and Social Affairs, Population Division, New York.

USGS (2016). Landsat 8 (L8) data users handbook. Department of the Interior U.S. Geological Survey.

Wu, C.D., Lung, S.C.C., Jan, J.F. (2013). Development of a 3-D urbanization index using digital terrain models for surface urban heat island effects. ISPRS J. Photogramm. Remote Sens., 81, 1–11.

Zhu, J., Tian, S., Tan, K., Du, P. (2016). Human settlement analysis based on multi-temporal remote sensing data: A case study of Xuzhou City, China. Chin. Geogr. Sci., 26, 389–400.